

Luminous AGB stars in nearby galaxies

A study using Virtual Observatory tools

P. Tsalmantza¹, E. Kontizas², L. Cambrésy³, F. Genova³, A. Dapergolas², and M. Kontizas¹

¹ Department of Astrophysics Astronomy & Mechanics, Faculty of Physics, University of Athens, GR-15783 Athens, Greece

² Institute for Astronomy and Astrophysics, National Observatory of Athens, P.O. Box 20048, GR-118 10 Athens, Greece

³ Observatoire Astronomique de Strasbourg, F-67000 Strasbourg, France

Received date / accepted

ABSTRACT

Aims. This study focuses on very luminous ($M_{\text{bol}} < -6.0$ mag) AGB stars with $J - K_s > 1.5$ mag and $H - K_s > 0.4$ mag in the LMC, SMC, M31, and M33 from 2MASS data.

Methods. The data were taken from the 2MASS All-Sky Point Source catalogue archive. We used Virtual Observatory tools and took advantage of its capabilities at various stages in the analysis.

Results. It is well known that stars with the colors we selected correspond mainly to carbon stars. Although the most luminous AGBs detected here contain a large number of carbon stars, they are not included in existing catalogues produced from data in the optical domain, where they are not visible since they are dust-enshrouded. A comparison of the AGB stars detected with combined near and mid-infrared data from MSX and 2MASS in the LMC shows that 10% of the bright AGB stars are bright carbon stars never detected before and that the other 50% are OH/IR oxygen rich stars, whereas the 40% that remain were not cross-matched.

Conclusions. The catalogues of the most luminous AGB stars compiled here are an important complement to existing data. In the LMC, these bright AGB stars are centrally located, whereas they are concentrated in an active star-formation ring in M31. In the SMC and M33, there are not enough of them to draw definite conclusions, although they tend to be centrally located. Their luminosity functions are similar for the four galaxies we studied.

Key words. – galaxies:individual: M31, M33, LMC, SMC – galaxies:local group – galaxies:photometry – stars:AGB

1. Introduction

The very red AGB stars, such as the various types of carbon and variable stars in galaxies, trace the intermediate-mass stellar population, thereby providing information about stellar evolution theories. Their spatial distribution is related to the star-formation history of the parent galaxy. These reddest and most extreme AGB stars cannot be detected easily at the conventional B , R wavelengths but can be observed in the near-infrared.

Carbon stars are detected in the optical domain if their mass is less than 4-5 M_{\odot} , whereas the more massive ones are expected to be seen only at longer wavelengths. Dredge-up and mass-loss determine whether an AGB star will become a carbon star. Very bright carbon stars can still be produced from stars with masses of 6 or 8 M_{\odot} , if the mass-loss rate is not too high to allow enough dredge-up episodes (Frost et al. 1998). Models of stars up to 6 M_{\odot} for solar and Magellanic metallicities have shown that all massive carbon stars are, or could be,

dust-enshrouded and should therefore not be visible at B and R wavelengths (Frost et al. 1998). In the near-infrared domain, where these stars are revealed best, carbon stars mainly populate the *red tail* (Nikolaev & Wenberg 2000 and Cioni et al. 2004), which is easily detected in the color-magnitude diagram M_{K_s} vs $J - K_s$ as an inclined branch of stars departing from an almost vertical sequence of red giants. It is not yet clear whether all stars in that area of the color-magnitude diagram are carbon stars. Marigo et al. (2003) point out that the majority of *red tail* stars are carbon, and Davidge (2003) showed that, in NGC 205, carbon stars are those among the *red tail* with the additional constraints $J - K_s > 1.5$ mag and $H - K_s > 0.4$ mag.

Adopting the above criteria for carbon stars, we selected carbon star candidates in the Magellanic Clouds, M31 and M33 galaxies from the 2MASS All-Sky Survey. The 2MASS detection limit allowed us to see only the brightest carbon star candidates in M31 and M33. On the other hand, the brightest carbon dust-enshrouded stars are not detected in the 4000-6000 Å range in which the published catalogues are based for both the SMC and LMC (Kontizas et al. 2001; Rebeiro et al. 1993; Morgan et al. 1995). Our search for the most luminous

AGB stars will produce a homogeneous set of data for all four galaxies as confined by the detection limit of 2MASS. Data retrieval and basic analysis were performed through the Virtual Observatory (VO) and relevant tools.

Although the most luminous AGB stars are expected to be carbon stars, a lack of carbon stars is observed for luminosities that are greater than $M_{\text{bol}} = -6.0$ mag (van Loon et al. 1991). One explanation is that luminous AGB stars become invisible at wavelengths shorter than $\approx 1 \mu\text{m}$ due to obscuration by a circumstellar dust shell as a result of intense mass loss on the TP-AGB (van Loon et al. 1991).

In the LMC cluster HS 327, there is evidence that carbon stars and OH/IR stars may be coeval (van Loon et al. 1991). These stars are most likely ≈ 200 Myr old and formed at an epoch of intense star formation in the LMC.

Egan et al. (2001), when combining 2MASS and MSX colors, studied the AGB population and other red stars in the LMC, including objects with unusual IR excesses. By using the IR point-source model by Wainscoat et al. (1992) and obtaining source names and spectral types from the SIMBAD database when available, they have identified 11 categories of stellar populations and red nebulae, including main-sequence stars, giant stars, red supergiants (RSGs), C- and O-rich AGB stars, PNs, HII regions, and other dusty objects likely associated with early-type stars. A total of 731 of these sources were previously unidentified. Comparing their results with the bright AGBs of the LMC studied here, we found that the majority of these stars are OH/IR and carbon stars.

In this study we provide the catalogues of the brightest AGB stars ($-8.4 < M_{\text{bol}} < -6.0$ mag) in four galaxies: the LMC, the SMC, M31, and M33. This selection of the magnitude range is due to the limit of detection of 2MASS in M31 and M33. The spatial distribution and corresponding luminosity functions are derived and discussed for each galaxy.

2. Data Analysis

2.1. VO tools

The recent developments of the Virtual Observatory create tools dedicated to some generic operations. Padovani et al. (2004) prove the efficiency of such tools in helping astronomers to produce scientific results using the European Astrophysical Virtual Observatory (AVO). We took advantage of the VO capabilities at various stages of the analysis presented in this paper. For instance, the CDS service VizieR (Ochsenbein et al. 2000) is used as an implicit cross-match tool to identify the LMC carbon stars from Kontizas et al. (2001) in the 2MASS point source catalogue. It is a positional cross-match that looks for sources within a maximum distance chosen by the user ($1''$ for this work). One of the main features of the VO is *interoperability*. VizieR output for 2MASS queries is directly displayed using VOPlot (Kale et al. 2004), a tool provided by the Indian VO. The interoperability between VizieR and VOPlot is ensured by the exchange of a VOTable¹ that makes it possible to directly visualize the spatial distribution or color-magnitude diagrams

resulting from the catalogue query. Moreover, the filtering capabilities of VOPlot allow one to use criteria to select and display a specific population, such as the AGB stars discussed in this paper. As an example, Fig. 8 shows the superposition of a color-filtered catalogue on the M31 GALEX image (Thilker et al. 2005). No WCS (World Coordinate System) information was initially available, but a registration could be obtained using Aladin (Bonnarel et al. 2000), which was the basis of the AVO prototype. There are still limitations in the VO tools. At the moment, for instance, very large catalogues cannot be handled in the same way as small catalogues. While the M31 catalogue (10^4 sources) is directly output in VOPlot, the LMC catalogue (2 million sources) is obtained via *vizquery*², which allows one to query VizieR remotely for further analysis.

2.2. AGB stars and Bolometric correction

The data used in this investigation were selected from the 2MASS all-sky survey catalogue restricted to objects for which the error is lower than 0.15 mag in all bands.

There are several criteria for detecting carbon stars in the various wavelengths. For the JHK_s filters the most conservative criteria are those by Davidge (2003), who found that stars with $H - K_s > 0.4$ mag and $J - K_s > 1.5$ mag in the galaxy NGC 205 are carbon stars. These color limits are known to be metallicity-dependent, with $J - K_s$ becoming redder by 0.1 mag when the metallicity changes from $Z=0.004$ to $Z=0.2$ (Davidge 2003). The metallicities of the four galaxies studied here are either similar or lower than the one studied by Davidge, which implies that the color $J - K_s$ can be bluer than the 1.5 mag value adopted here. If taking the metallicity effect into consideration, our sample might not include some of the bluest stars. Considering that the upper part of the red tail contains C-rich, O-rich, OH/IR stars, only spectra would be able to solve the ambiguity about the nature of these bright red stars.

To compare the results found here with previous studies of the carbon star populations in galaxies, the K_s magnitudes of the stars were converted into bolometric magnitudes. The bolometric correction used is an approximation proposed by Bessel & Wood (1984). Some more recent references are actually based on a similar assumption. Bessel & Wood (1984) computed the bolometric correction, BC_K , in the K magnitude for various AGB stars in the Galaxy, LMC, SMC, and 47 Tuc. The available carbon star observations were too few to deduce a relation for them alone, but it was found that the O-rich stars' relation for M_{bol} describes well the few carbon stars in the $H - K$ vs $J - K$ diagram. In this same study it was shown that the bolometric corrections vary for stars in galaxies with different metallicities. For stars in the Galaxy and LMC, the correction given by Bessel & Wood (1984) is $BC_K = 0.72 + 2.65 \times (J - K) - 0.67 \times (J - K)^2$, which was validated for the magnitude range $0.6 < J - K < 2.0$ mag. This is the correction we used for the LMC, but also for M31 and M33, considering that they have the same metallicity as the Galaxy and LMC respectively. For stars in the SMC, the correction found by Bessel & Wood (1984) was $BC_K = 0.60 + 2.65 \times (J - K) - 0.67 \times (J - K)^2$

¹ <http://www.ivoa.net>

² <http://cdsweb.u-strasbg.fr/doc/vizquery.htx>

for stars with $0.6 < J - K < 1.5$ mag. Beyond that color limit no data were available in the SMC, so in this case we used the bolometric corrections for stars in the LMC as an approximation. This might lead to calculated values of M_{bol} that are higher than the real ones for the SMC stars, but the difference between the two formulae is only 0.1 mag. This result is also supported by Montegriffo et al. (1998) who studied the bolometric corrections in several Galactic globular clusters with various metallicities. They found that the bolometric corrections for metal-poor objects are very close to those calculated from the metal-rich relation at redder colors.

3. Color–magnitude diagrams

3.1. The Large Magellanic Cloud

Modeling the color–magnitude diagram of the *red tail* of the LMC from the 2MASS data, Marigo et al. (2003) found that field stars are not expected to reach colors that are redder than $J - K_s \approx 1.0$ mag, thus they hardly contaminate the features produced by the LMC population of AGB stars. We assumed the distance modulus $m - M = 18.55 \pm 0.04(\text{statistical}) \pm 0.08(\text{systematic})$ mag (Cioni et al. 2004) and the mean reddening $E_{B-V} = 0.13$ mag (Massey et al. 1995), which gives an absorption of $A_{K_s} = 0.04$ mag using $A_{K_s} = 0.34 \times E_{B-V}$ (Bessel & Brett 1988). Carbon star candidates were selected following Davidge criteria (2003) in the 2MASS M_{K_s} vs $J - K_s$ diagram presented in Fig 1. Keeping only objects with 2MASS photometric errors less than 0.15 mag, we found 7137 carbon star candidates among the 10055 stars that belong to the *red tail*, which is defined by $J - K_s > 1.3$ mag and $M_{K_s} < -6.5$ mag (Cioni et al. 2004). The cross–match within a $3''$ radius of the 7137 AGB stars with the 7716 spectroscopically confirmed carbon stars from Kontizas et al. (2001) gives 3782 common objects. This confirms that *red tail* stars contain a large number of carbon stars.

A comparison with Kontizas et al. (2001) data shows that the bright end of the optically detected carbon stars is two magnitudes fainter in the near–infrared than the bright end of the *red tail* stars detected in 2MASS. The bright AGB stars with $-8.4 < M_{\text{bol}} < -6.0$ mag are found to be 216 (Table A.1), whereas the total number of the bright *red tail* stars is 256. In addition, we searched the DSS catalogue in three colors $B(J)$, R , and I to confirm that these stars are not observable in the B , R wavelengths. We found that many stars (almost 1 out of 5) are not visible in B and R (traditionally accepted as the representative optical window), but they become detectable or appear very luminous in I , as shown in the example of Fig. 2. Deep surveys may reveal these stars, but available observations have not detected them yet.

The spatial distribution of the 7137 *red tail* AGB stars extracted from 2MASS is presented at the top of Fig. 3, and the bottom figure shows the distribution of the 216 most luminous of them. Figure 3 shows high density in the central regions for the *red tail* AGB stars, including the most luminous ones, in agreement with previous studies by Hughes & Wood (1990) and Wood et al. (1985).

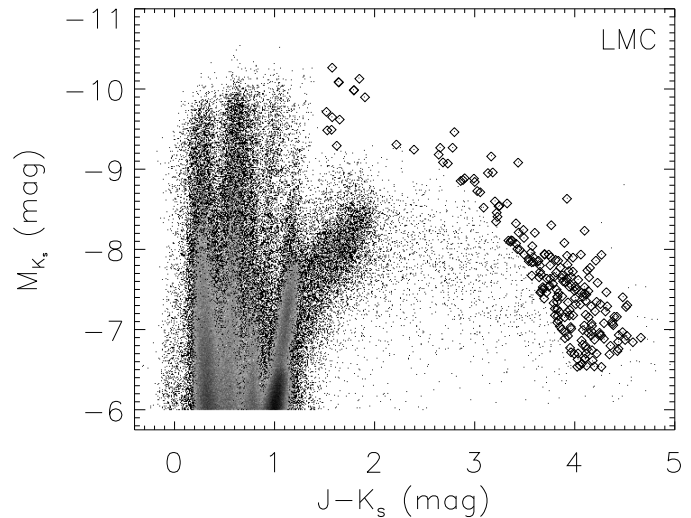


Fig. 1. Color–magnitude diagram for the LMC stars with $M_{K_s} < -6.0$ mag. The *red tail* is defined by $J - K_s > 1.3$ mag and $M_{K_s} < -6.5$ mag, whereas the luminous AGB stars with $-8.4 < M_{\text{bol}} < -6.0$ mag are shown with diamonds

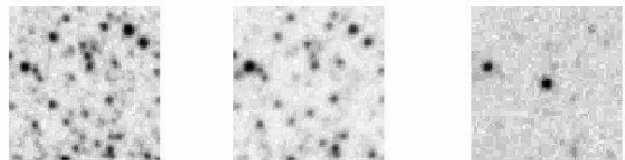


Fig. 2. The $B(J)$, R , I images from the DSS survey of one LMC carbon star detected here (2MASS J04532183-7051449) show that it is only detected in the I band.

Egan et al. (2001) combined LMC data from 2MASS and MSX to detect carbon stars. They defined carbon stars by using the criteria $1.5 < K_s - A < 3.75$ mag and $0.8 < H - K_s < 1.5$ mag and the OH/IR with $J - K_s > 3$ mag, $K_s - A > 3.75$ mag and $H - K_s > 1.5$ mag. Cross–matching the stars found here with those of Egan et al. (2001) has shown that 20 of the luminous AGB stars are actually carbon stars, 109 of them are OH/IR stars, 5 are planetary nebulae, 1 is oxygen–rich AGB and 1 is carbon–rich AGB star, 24 are of unknown nature, and no match was found for the 56 other stars included in our sample.

3.2. The Small Magellanic Cloud

Like the LMC, no significant foreground star contamination is expected at $J - K_s > 1.0$ mag (Marigo et al. 2003) toward the SMC. The distance modulus is $m - M = 18.99 \pm 0.03(\text{statistical}) \pm 0.08(\text{systematic})$ mag (Cioni et al. 2004). The mean reddening adopted here is the one given by Massey et al. (1995) $E_{B-V} = 0.09$ mag, which corresponds to $A_{K_s} = 0.03$ mag. The *red tail* known to be located at $J - K_s > 1.2$ mag and $M_{K_s} < -7.0$ mag can be seen in Fig. 4. It contains 1674

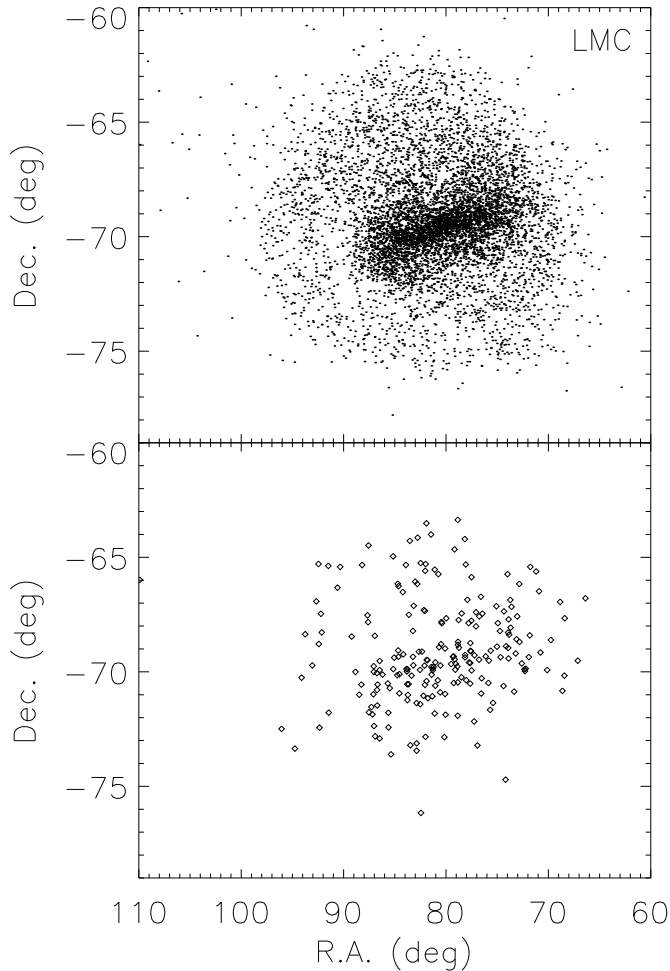


Fig. 3. Spatial distribution of all LMC AGB stars selected in this paper (top), and the very bright ones with $-8.4 < M_{\text{bol}} < -6.0$ mag (bottom).

stars in the 2MASS catalogue when restricted to sources with photometric errors smaller than 0.15 mag. Among them, 911 are carbon star candidates if assuming the Davidge (2003) criteria. There are 34 bright carbon stars with $-8.4 < M_{\text{bol}} < -6.0$ mag (Table A.2) out of a total of 50 bright sources in the *red tail*. A $3''$ radius cross-match of the 911 carbon star candidates with the catalogues of SMC carbon stars confirmed by spectroscopy in the optical wavelengths (Rebeiro et al. 1993; Morgan et al. 1995) gives 676 sources in common. It is worth noting that only one cross-matched star belongs to the 34 very bright AGB stars of our sample.

The carbon star candidates selected here are distributed within an elliptical area, with no obvious central concentration (Fig. 5). The brightest sources with $-8.4 < M_{\text{bol}} < -6.0$ mag tend to be in the central area, although they are too few in number to draw a definite conclusion. Demers et al. (2003) found that the carbon stars are located almost exclusively in and near the disk for the Magellanic type galaxy NGC 3109. This is consistent with our results in the SMC and the LMC.

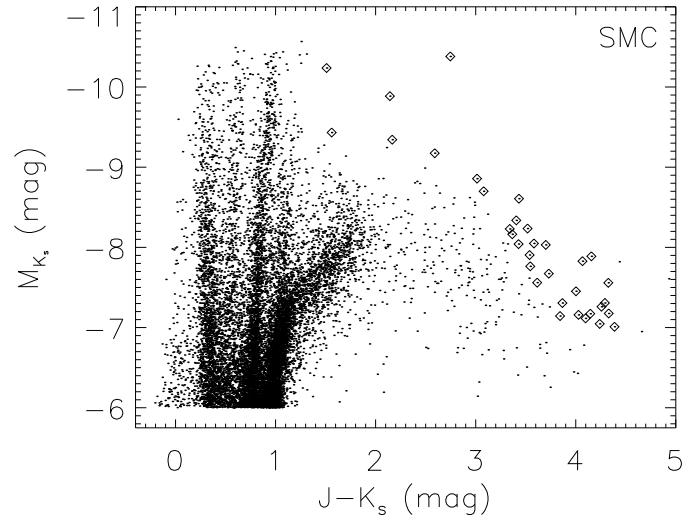


Fig. 4. Color-magnitude diagram for all SMC stars with $M_{K_s} < -6.0$ mag. The *red tail* is defined by $J - K_s > 1.2$ mag and $M_{K_s} < -7.0$ mag, whereas the luminous AGB stars with $-8.4 < M_{\text{bol}} < -6.0$ mag are shown with diamonds.

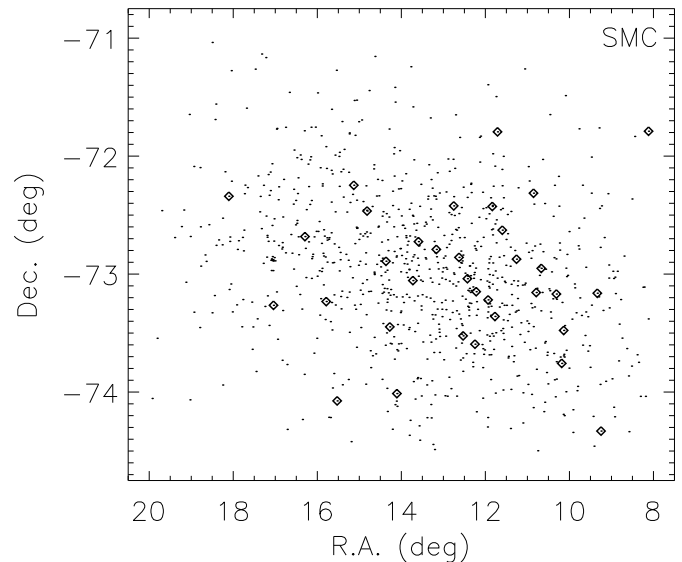


Fig. 5. Spatial distribution of all SMC AGB stars selected in this paper (dots). The most luminous with $-8.4 < M_{\text{bol}} < -6.0$ mag are represented with diamonds.

3.3. Messier 31

M31 is a more distant galaxy than the LMC and SMC, with a distance modulus of $m - M = 24.38 \pm 0.05$ mag (Brewer and Richer 1995). The color-magnitude diagram presented in Fig. 6 shows that only the upper part of the *red tail* is observable in M31 because of the 2MASS sensitivity limit. It was assumed that all $J - K_s \geq 1.1$ mag stars are *red tail* stars (see Fig. 6). In that area there are 959 stars with photometric errors less than 0.15 mag. Since M31 is located at an intermediate galactic latitude, the question of foreground star contamination

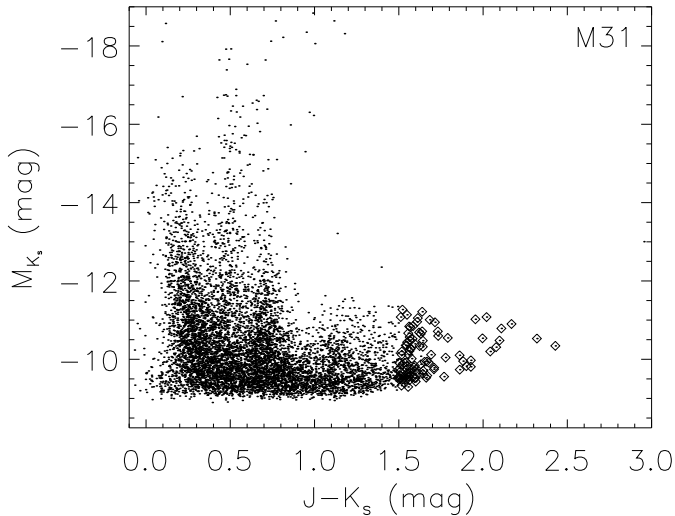


Fig. 6. Color–magnitude diagram for all M31 stars detected by 2MASS. The upper part of the *red tail* is located at $J - K_s > 1.1$ mag, whereas the luminous AGB stars with $-8.4 < M_{\text{bol}} < -6.0$ mag are shown with diamonds.

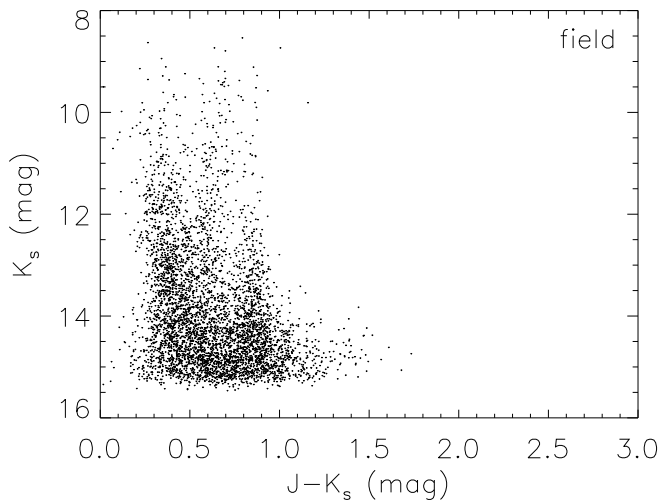


Fig. 7. Color–magnitude diagram for stars detected by 2MASS in a nearby field.

needs to be properly addressed. We retrieved data from a region near M31 (Fig. 7), located at $16.0 < \text{RA} < 17.5$ deg and $40.5 < \text{Dec} < 42.0$ deg. The color–magnitude diagram for M31 is very populated at $J - K_s > 1.1$ mag (Fig. 6), whereas the neighboring field (Fig. 7) contains very few stars in this part of the diagram, indicating that the contamination from the Milky Way stellar population is very low.

For the total reddening correction near M31, $E_{B-V} \approx 0.23$ mag is adopted (Brewer & Richer 1995). Consequently the absorption at K_s is 0.08 mag, assuming again $A_{K_s} = 0.34 \times E_{B-V}$ (Bessel & Brett 1988). From these relatively low absorption values, we excluded the possibility that the 959 *red tail* stars are early type stars heavily obscured, although they are located in the spiral structure of M31.

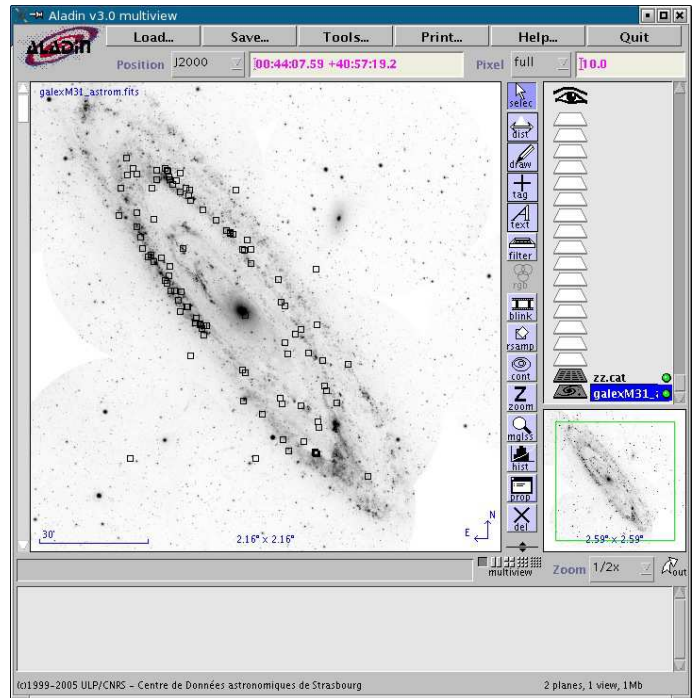


Fig. 8. The brightest carbon star candidates found in M31 (squares) overplotted on the GALEX UV image, as processed by Aladin v3.0.

Considering the criteria of Davidge (2003), only 100 stars are carbon star candidates. In Fig. 8 we overplotted the carbon star candidates found in M31 on the GALEX image. These stars fall on the star forming regions detected at UV wavelengths, following the familiar M31 ring–structure, 10 kpc away from the galaxy center. This ring has been detected in most of the large scale maps at radio wavelengths (Beck & Gräve 1982; Brinks & Shane 1984), and is also traced by star-forming regions (Pellet et al. 1978; Devereux et al. 1994). This structure can also be noted in the infrared (Haas et al. 1998), in the optical via masking (Walterbos & Kennicutt 1988), and in the distribution of HII regions (Pellet et al. 1978), OB associations (van der Bergh 1991), HI gas (Sofue & Kato 1981), and other tracers (see Hodge 1992). The spatial distribution of the carbon star candidates suggests that the velocity dispersion and the differential galactic rotation have not had enough time to spread these bright AGB stars, which are among the youngest intermediate mass stars produced in spiral arms, like the current population of young stars. All the 100 bright AGB stars detected here are within the magnitude range of $-8.4 < M_{\text{bol}} < -6.0$ mag. They are listed in Table A.3.

In previous investigations of carbon stars in M31, either the studied areas are far from the ring of luminous AGB stars presented in this paper or candidate carbon stars are fainter (Brewer et al. 1996; Battinelli et al. 2003; Battinelli et al. 2005; Davidge et al. 2005).

3.4. Messier 33

To complete our survey of the brightest *red tail* stars in nearby galaxies, we took the 2MASS data for M33 and followed the

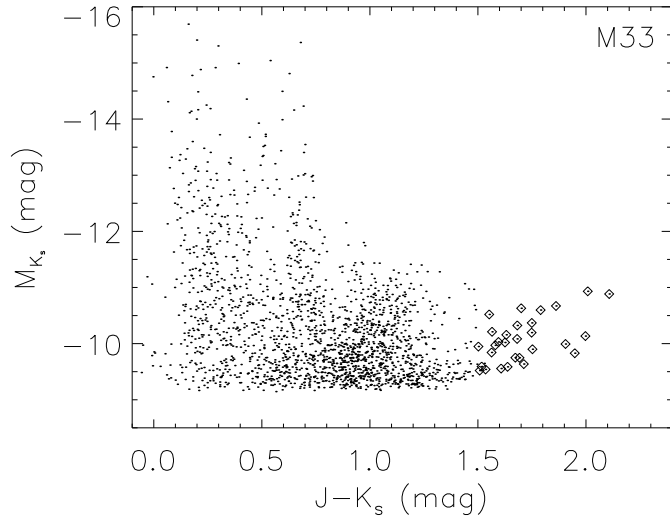


Fig. 9. Color–magnitude diagram for the stars in M33. The upper part of the *red tail* is located at $J - K > 1.0$ mag, whereas the luminous AGB stars with $-8.4 < M_{\text{bol}} < -6.0$ mag are shown with diamonds.

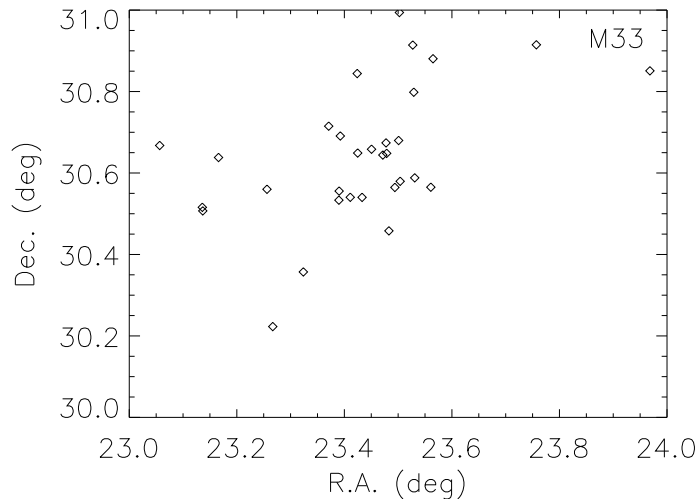


Fig. 10. Spatial distribution of the most luminous AGB stars with $-8.4 < M_{\text{bol}} < -6.0$ mag.

same process as for the LMC, SMC, and M31. Wilson et al. (1991) derive $E_{B-V} = 0.3 \pm 0.1$, including both the Milky Way foreground and M33 internal extinction. This color excess is translated into $A_{K_s} \approx 0.10$ mag. The distance modulus for M33 is $m - M = 24.52 \pm 0.14$ (statistical) ± 0.13 (systematic) mag (Lee et al. 2002), and the *red tail* is located at $J - K_s > 1.0$ mag (Fig. 9). Block et al. (2004) consider that stars detected by 2MASS with $J - K_s > 1.0$ mag cannot be M-stars in the low-metallicity regions, indicating the presence of *red tail* stars. In this area of the color–magnitude diagram, 916 stars have been found; and among them, 31 are supposed to be carbon stars, after we adopt the Davidge (2003) criteria. We stress that all the 31 carbon star candidates are very bright with $-8.4 < M_{\text{bol}} < -6.0$ mag (see Table A.4).

The spatial distribution of these stars (Fig. 10) is not correlated with the arcs of red stars found by Block et al. (2004) in the disk of M33. The cross-identification of these 31 carbon star candidates with those of Rowe et al. (2005) gives no pair within a $1''$ search radius. Their study has not revealed the most luminous AGB star population detected in our paper here, most probably because their observations are in the optical domain where these stars are not detected.

4. Discussion and conclusion

4.1. Luminosity Functions

The luminosity function reflects the distribution of stellar masses formed in a given volume of space for a stellar system or a galaxy. The upper end of the luminosity function displays the most massive stars of any particular population. Carbon stars usually have intermediate mass and provide insight into the star-forming history of these masses.

The luminosity function for the bright AGBs in each galaxy is presented in Fig. 11 (LMC, SMC, M31, M33). It illustrates that in all four galaxies, luminous carbon and OH/IR candidates (Egan et al. 2001) exhibit a similar luminosity function with slopes varying only slightly and within the errors of the fit. This result suggests that a similar mass distribution is expected in all four galaxies for the upper part of the mass function. Groenewegen (2002) found that the faint part of luminosity functions are also similar. Luminosity functions for the bright *red tail* population are presented in Fig. 12. No significant difference is found between the population of bright ($-8.4 < M_{\text{bol}} < -6.0$ mag) AGB *red tail* stars ($H - K_s > 0.4$ mag and $J - K_s > 1.5$ mag) and the whole population of *red tail* stars (LMC: $J - K_s > 1.3$ mag and $M_{K_s} < -6.5$ mag, SMC: $J - K_s > 1.2$ mag and $M_{K_s} < -7.0$ mag, M31: $J - K_s > 1.1$ mag, M33: $J - K_s > 1.0$ mag).

4.2. The spatial distribution

In the present work the spatial distribution of the luminous AGB stars appears to depend on the environment. In the LMC they are distributed within an ellipse defined by the extent of the old population of the galaxy. The density is higher along the bar, while the most luminous AGB stars are concentrated in the central area where the young cluster systems are located (Kontizas et al., 1993, Kontizas et al., 1993).

In M31 the AGB stars are distributed on the spiral features of the galaxy. Therefore both the LMC and M31 show that the luminous and, consequently, the most massive AGB stars trace the location of the star-forming regions of their parent galaxy. On the other hand, the less massive stars that evolve slowly have the time to reach the outer parts of the galaxy, as observed for the LMC. To confirm this behavior in M31, deeper near-infrared data are required.

In the SMC and M33, AGBs are located in an elliptical area along the disk, without an obvious higher density at star-forming regions, i.e. the center and the spiral structure. It is difficult to draw any conclusion from this diagrams since the

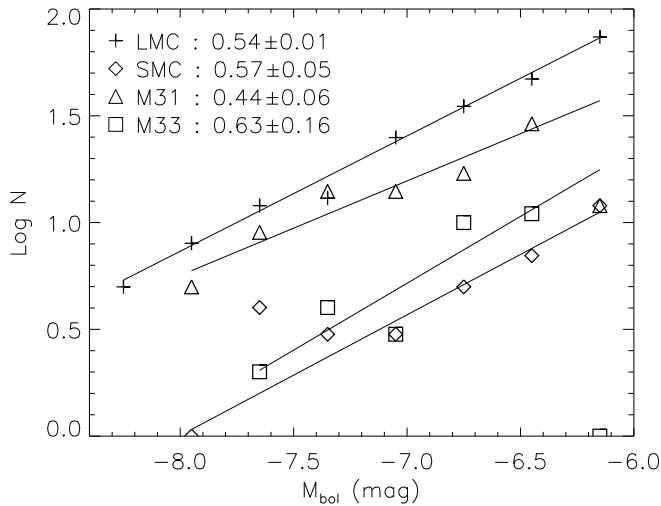


Fig. 11. Luminosity functions for the luminous carbon and OH/IR candidates found in the LMC, the SMC, M31, and M33. Numbers in the upper-left corner are the slopes of the linear regression fits.

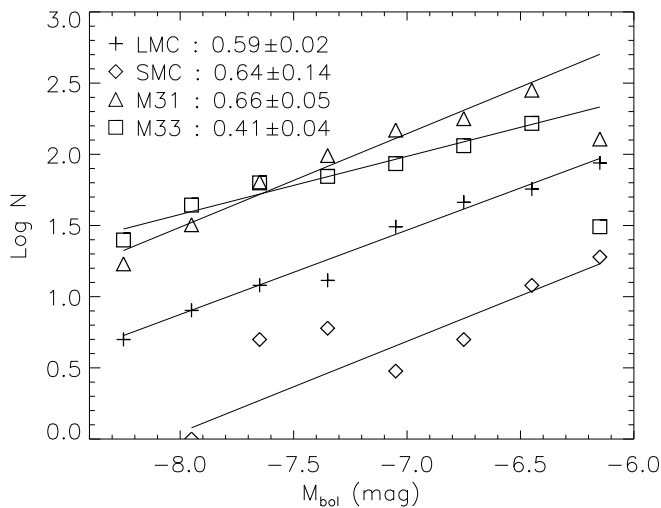


Fig. 12. Luminosity function for the bright *red tail* stars found in the LMC, the SMC, M31, and M33. Numbers in the upper-left corner are the slopes of the linear regression fits.

amount of luminous AGB stars detected in these galaxies is very small.

4.3. Conclusion

We searched for the most luminous AGB stars in four nearby galaxies: the LMC, the SMC, M31, and M33. Stars were selected on the *red tail* of the color-magnitude diagram (M_{K_s} , $J - K_s$) with $J - K_s > 1.5$ mag and $H - K_s > 0.4$ mag. Known optical catalogues of carbon stars in the SMC and LMC do not include these luminous AGB stars, since they were constructed from observations at *B* and *R* wavelengths; therefore, the cat-

alogues of luminous AGB stars compiled in this work are a valuable complement to existing data.

Using the same range in M_{bol} ($-8.4 < M_{bol} < -6.0$ mag) for the four galaxies, we analyzed the spatial distribution of these stars. We found that they follow the spiral ring of M31 and are mostly located in the central region of the LMC, where all the young population is concentrated. In the SMC and in M33, their number is too small to draw reliable conclusions about their location. Finally the luminosity functions of the *red tail* stars and the bright AGB stars, display similar slopes within the same bolometric magnitude range.

5. Acknowledgments

The authors would like to thank the CDS and the VO for valuable support. P. Tsalmantza and M. Kontizas would like to thank the E.L.K.E. of the University of Athens and the Greek General Secretariat of Research & Technology. Special thanks go to the University of Strasbourg for financial support and the hospitality of E. & M. Kontizas. This publication makes use of data products from the Two Micron All Sky Survey, which is a joint project of the University of Massachusetts and the Infrared Processing and Analysis Center/California Institute of Technology, funded by the National Aeronautics and Space Administration and the National Science Foundation. This research made use of the VizieR catalogue access tool and Aladin, CDS, Strasbourg, France. Finally, but not least, we would like to thank the unknown referee for very constructive and stimulating comments.

References

- Battinelli, P., Demers, S., 2005, *A&A*, 430, 905
- Battinelli, P., Demers, S., Letarte, B., 2003, *AJ*, 125, 1298
- Beck, R., Gräve, R., 1982, *A&A*, 105, 192
- Bessell, M. S., Brett, J. M., 1988, *PASP*, 100, 1134
- Bessell, M. S., Wood, P. R., 1984, *PASP*, 96, 247
- Block, D. L., Freeman, K. C., Jarrett, T. H., Puerari, I., Worthey, G., Combes, F., Groess, R., 2004, *A&A*, 425, L37
- Bonnarel, F., Fernique, P., Bienaymé, O., Egret, D., Genova, F., Louys, M., Ochsenbein, F., Wenger, M., Bartlett, J. G., 2000, *A&AS*, 143, 33
- Brewer, J. P., Richer, H. B., Crabtree, D. R., 1996, *AJ*, 112, 491
- Brewer, J. P., Richer, H. B., Crabtree, D. R., 1995, *AJ*, 109, 2480
- Brinks, E., Shane, W. W., 1984, *A&AS*, 55, 179
- Cioni, M. R. L., Habing, H. J., Loup, C., Epchtein, N., Deul, E., 2004, *Msngr*, 115, 22
- Davidge, T. J., Olsen, K. A. G., Blum, R., Stephens, A. W., Rigaut, F., 2005, *AJ*, 129, 201
- Davidge, T. J., 2003, *ApJ*, 597, 289
- Demers, S., Battinelli, P., Letarte, B., 2003, *A&A*, 410, 795
- Devereux, N. A., Price, R., Wells, L. A., Duric, N., 1994, *AJ*, 108, 1667
- Egan, M. P., Van Dyk, S. D., Price, S. D., 2001, *AJ*, 122, 1844
- Frost, C. A., Cannon, R. C., Lattanzio, J. C., Wood, P. R., Forestini, M., 1998, *A&A*, 332, L17
- Groenewegen, M. A. T., 2002, *astro-ph/0208449*
- Haas, M., Lemke, D., Stickel, M., Hippelein, H., Kunkel, M., Herbstmeier, U., Mattila, K., *A&A*, 1998, 338, L33
- Hodge, P., 1992, *The Andromeda Galaxy*, Kluwer Academic Publishers, Dordrecht

- Hughes, S. M. G., Wood, P. R., 1990, *AJ*, 99, 784
- Kale, S., Vijayaraman, T. M., Kembhavi, A., Krishnan, P. R., Navelkar, A., Hegde, H., Kulkarni, P., & Balaji, K. D. 2004, *Astronomical Society of the Pacific Conference Series*, 314, 350
- Kontizas, E., Dapergolas, A., Morgan, D. H., Kontizas, M., 2001, *A&A*, 369, 932
- Kontizas, M., Kontizas, E., Michalitsianos, A. G., 1993, *A&A*, 269, 107
- Lee, M. G., Kim, M., Sarajedini, A., Geisler, D., Gieren, W., 2002, *ApJ*, 565, 959
- Marigo, P., Girardi, L., Chiosi, C., 2003, *A&A*, 403, 225
- Massey, P., Lang, C. C., Degioia-Eastwood, K., Garmany, C. D., 1995, *ApJ*, 438, 188
- Montegriffo, P., Ferraro, F. R., Origlia, L., Fusi Pecci, F., 1998, *MNRAS*, 297, 872
- Morgan, D. H., Hatzidimitriou, D., 1995, *A&AS*, 113, 539
- Nikolaev S. and Weinberg M. D., 2000, *ApJ*, 542, 804
- Ochsenbein, F., Bauer, P., Marcout, J., 2000, *A&AS*, 143, 23
- Padovani, P., AVO, 2004, AAS, 20513006
- Pellet, A., Astier, N., Viale, A., Courtes, G., Maucherat, A., Monnet, G., Simien, F., 1978, *A&AS*, 31, 439
- Rebeiro, E., Azzopardi, M., Westerlund, B. E., 1993, *A&AS*, 97, 603
- Richer, H. B., 1989, *IAU Coll. 106*, (Cambridge University Press), 35
- Rowe, J. F., Richer, H. B., Brewer, J. P., Crabtree, D. R., 2005, *AJ*, 129, 729
- Sofue, Y., Kato, T., 1981, *Publ. Astron. Soc. Japan*, 33, 449
- Thilker, D. A., Hoopes, C. G., Bianchi, L., Boissier, S., Rich, R. M., Seibert, M., Friedman, P. G., Rey, S. C., Buat, V., Barlow, T. A. and 18 coauthors 2005, *ApJ*, 619L, 67
- van den Bergh, S., 1991, *PASP*, 103, 1053
- van Loon, J. Th., Zijlstra, A. A., Kaper, L., Gilmore, G. F., Loup, C., Blommaert, J. A. D. L., 2001, *A&A*, 368, 239
- Wainscoat, R. J., Cohen, M., Volk, K., Walker, H. J., Schwartz, D. E., 1992, *ApJS*, 83, 111
- Walterbos, R. A. M., Kennicutt, R. C, Jr., 1988, *A&A*, 198, 61
- Wilson, C. D., 1991, *AJ*, 101, 1663
- Wood, P. R., Bessell, M. S., Paltoglou, G., 1985, *ApJ*, 290, 477

Appendix A: Tables

Table A.1. Very luminous AGB stars (carbon star candidates) in the LMC

2MASS ID	RA (deg)	Dec (deg)	M_K (mag)	M_{bol} (mag)	$J - K_s$ (mag)
2MASS J06103966-6655227	92.665289	-66.922974	-6.639	-6.323	4.10
2MASS J06022433-6619263	90.601393	-66.323982	-7.723	-7.073	3.98
2MASS J05294752-7609256	82.448038	-76.157127	-7.677	-6.752	3.88
2MASS J04564410-7442267	74.183760	-74.707420	-7.638	-6.831	3.92
2MASS J06011982-6525021	90.332610	-65.417274	-7.844	-6.238	3.59
2MASS J06055819-6522162	91.492478	-65.371185	-7.392	-6.798	4.00
2MASS J06094920-6517197	92.455038	-65.288811	-6.541	-6.496	4.20
2MASS J05412924-7336038	85.371848	-73.601082	-7.331	-6.190	3.79
2MASS J05312948-7326331	82.872862	-73.442551	-7.010	-6.314	3.96
2MASS J05074394-7312521	76.933107	-73.214478	-7.318	-7.460	4.26
2MASS J05335481-7312143	83.478390	-73.203995	-6.979	-6.857	4.17
2MASS J05312710-7307148	82.862936	-73.120804	-7.485	-6.878	4.00
2MASS J05455697-7254291	86.487392	-72.908104	-7.530	-6.134	3.68
2MASS J05203823-7251062	80.159310	-72.851723	-7.644	-6.709	3.87
2MASS J05280053-7250120	82.002241	-72.836685	-7.038	-6.050	3.85
2MASS J05474046-7248485	86.918596	-72.813484	-6.843	-8.045	4.58
2MASS J05422827-7225333	85.617810	-72.425926	-7.652	-6.173	3.64
2MASS J05480721-7221516	87.030047	-72.364342	-6.636	-6.315	4.10
2MASS J05085905-7209546	77.246083	-72.165176	-7.452	-7.116	4.10
2MASS J05152480-7154493	78.853353	-71.913696	-6.927	-7.090	4.26
2MASS J05200955-7152132	80.039798	-71.870346	-6.927	-6.793	4.17
2MASS J05484335-7151165	87.180628	-71.854607	-7.178	-6.536	3.98
2MASS J05242503-7149020	81.104331	-71.817238	-7.547	-6.862	3.97
2MASS J05423112-7146588	85.629679	-71.783005	-7.226	-7.522	4.31
2MASS J05500676-7146026	87.528169	-71.767410	-7.536	-6.950	4.01
2MASS J06190234-7321026	94.759790	-73.350746	-6.923	-7.918	4.52
2MASS J05024447-7139323	75.685300	-71.658974	-7.097	-7.602	4.37
2MASS J05490888-7132069	87.287000	-71.535255	-9.085	-6.078	2.68
2MASS J05465088-7128033	86.712036	-71.467598	-6.871	-7.805	4.50
2MASS J05300380-7124361	82.515852	-71.410049	-6.690	-7.112	4.35
2MASS J05313006-7121448	82.875254	-71.362465	-7.869	-6.774	3.81
2MASS J05013788-7121123	75.407859	-71.353432	-7.305	-8.313	4.53
2MASS J05350379-7113576	83.765795	-71.232681	-7.885	-6.174	3.54
2MASS J05270395-7108591	81.766488	-71.149750	-7.898	-7.250	3.98
2MASS J06241389-7229196	96.057905	-72.488785	-9.307	-6.005	2.22
2MASS J05251951-7104027	81.331302	-71.067429	-7.859	-7.861	4.21
2MASS J06092546-7226037	92.356121	-72.434364	-7.846	-6.333	3.63
2MASS J05284817-7102289	82.200709	-71.041374	-8.713	-6.151	3.06
2MASS J05345289-7100229	83.720388	-71.006363	-8.853	-6.035	2.86
2MASS J05535326-7059475	88.471917	-70.996529	-7.462	-6.149	3.72
2MASS J05482201-7058476	87.091717	-70.979904	-7.802	-6.577	3.75
2MASS J05202105-7057545	80.087720	-70.965149	-7.620	-7.114	4.03
2MASS J05061466-7056427	76.561102	-70.945198	-6.701	-6.724	4.22
2MASS J05381238-7056174	84.551612	-70.938194	-6.967	-6.109	3.90
2MASS J05221654-7053460	80.568919	-70.896126	-7.635	-6.332	3.72

table continuation

2MASS ID	RA (deg)	Dec (deg)	M_K (mag)	M_{bol} (mag)	$J - K_s$ (mag)
2MASS J04532183-7051449	73.340999	-70.862488	-7.933	-8.105	4.27
2MASS J04343118-7049491	68.629954	-70.830322	-6.548	-6.278	4.12
2MASS J05465510-7047254	86.729615	-70.790390	-7.808	-7.017	3.93
2MASS J06054883-7146462	91.453467	-71.779518	-7.313	-6.865	4.06
2MASS J05415782-7042418	85.490917	-70.711617	-7.710	-6.627	3.81
2MASS J04573049-7036575	74.377079	-70.615990	-8.211	-6.302	3.44
2MASS J05241094-7036210	81.045601	-70.605843	-8.243	-6.430	3.49
2MASS J05281148-7033586	82.047840	-70.566299	-6.704	-6.192	4.03
2MASS J05530336-7033172	88.264027	-70.554779	-9.082	-7.163	3.43
2MASS J05464319-7033154	86.679960	-70.554283	-7.032	-6.325	3.96
2MASS J05350751-7032195	83.781320	-70.538757	-7.798	-6.337	3.65
2MASS J05343646-7032135	83.651938	-70.537094	-6.577	-6.176	4.07
2MASS J05103253-7030497	77.635542	-70.513832	-8.302	-7.103	3.77
2MASS J05424425-7030208	85.684407	-70.505783	-7.175	-6.434	3.95
2MASS J05032665-7029090	75.861058	-70.485855	-7.256	-6.203	3.83
2MASS J05165826-7029085	79.242791	-70.485703	-8.072	-6.113	3.41
2MASS J05152170-7027315	78.840457	-70.458771	-7.904	-6.295	3.59
2MASS J06162403-7015127	94.100149	-70.253555	-6.772	-6.047	3.95
2MASS J05273669-7024036	81.902897	-70.401024	-7.186	-6.890	4.11
2MASS J05231239-7022045	80.801638	-70.367935	-7.657	-6.528	3.79
2MASS J05120517-7021582	78.021575	-70.366173	-7.155	-6.945	4.14
2MASS J06121430-6943119	93.059601	-69.719978	-6.535	-6.704	4.27
2MASS J05060423-7016513	76.517648	-70.280930	-10.087	-6.823	1.64
2MASS J06094093-6847002	92.420551	-68.783401	-8.081	-7.207	3.90
2MASS J05135752-7014104	78.489704	-70.236237	-7.903	-6.689	3.76
2MASS J06083184-6816353	92.132673	-68.276482	-6.743	-6.633	4.17
2MASS J05332717-7009516	83.363228	-70.164352	-6.893	-6.035	3.90
2MASS J04334368-7009504	68.432034	-70.164024	-6.696	-6.089	4.00
2MASS J05390173-7008429	84.757222	-70.145256	-7.737	-7.490	4.13
2MASS J05253612-7007235	81.400528	-70.123215	-8.346	-6.029	3.21
2MASS J05444714-7007047	86.196438	-70.117973	-7.499	-6.094	3.68
2MASS J05381127-7006088	84.546982	-70.102470	-9.649	-6.417	1.58
2MASS J05470053-7003170	86.752248	-70.054733	-7.347	-7.370	4.22
2MASS J05481114-7000167	87.046428	-70.004646	-6.551	-6.092	4.05
2MASS J05552103-7000030	88.837643	-70.000847	-9.463	-6.573	2.80
2MASS J05351559-6958443	83.814974	-69.978996	-7.858	-6.365	3.64
2MASS J04491008-6958048	72.292016	-69.968002	-7.674	-6.033	3.57
2MASS J05095999-6956097	77.499982	-69.936028	-8.574	-6.449	3.32
2MASS J05250941-6955407	81.289231	-69.927994	-8.887	-6.116	2.90
2MASS J05455416-6955172	86.475667	-69.921448	-7.997	-6.108	3.45
2MASS J04402848-6955135	70.118687	-69.920441	-9.897	-6.560	1.90
2MASS J05300859-6954496	82.535810	-69.913795	-8.537	-6.263	3.24
2MASS J05162261-6954181	79.094245	-69.905037	-7.687	-6.250	3.66
2MASS J04491848-6953145	72.327023	-69.887367	-9.159	-6.764	3.17
2MASS J05403606-6952498	85.150270	-69.880508	-8.233	-7.906	4.10
2MASS J05350354-6952454	83.764785	-69.879295	-7.936	-7.505	4.06
2MASS J05352686-6952279	83.861930	-69.874420	-7.536	-6.787	3.94
2MASS J04485265-6951334	72.219410	-69.859299	-7.282	-8.246	4.51
2MASS J05251232-6950377	81.301366	-69.843819	-8.325	-6.364	3.41
2MASS J05254237-6947129	81.426567	-69.786942	-7.170	-6.132	3.83
2MASS J05245135-6947042	81.213967	-69.784508	-8.109	-6.079	3.38
2MASS J05153398-6945590	78.891600	-69.766396	-7.161	-7.737	4.40

table continuation

2MASS ID	RA (deg)	Dec (deg)	M_K (mag)	M_{bol} (mag)	$J - K_s$ (mag)
2MASS J05481349-6945115	87.056240	-69.753204	-7.229	-7.208	4.20
2MASS J05282342-6943387	82.097615	-69.727425	-6.849	-7.552	4.43
2MASS J05220985-6943200	80.541050	-69.722244	-7.934	-6.580	3.70
2MASS J05324622-6942497	83.192614	-69.713829	-8.458	-6.152	3.22
2MASS J05175887-6939231	79.495332	-69.656433	-9.485	-6.281	1.53
2MASS J05161189-6938596	79.049581	-69.649895	-7.222	-6.224	3.85
2MASS J04502338-6937567	72.597436	-69.632431	-7.458	-7.046	4.07
2MASS J05103243-6936542	77.635141	-69.615059	-7.572	-6.414	3.78
2MASS J05105680-6935303	77.736668	-69.591759	-7.584	-7.638	4.23
2MASS J05240917-6935112	81.038249	-69.586456	-9.071	-6.111	2.73
2MASS J05455384-6931233	86.474335	-69.523140	-9.492	-6.263	1.57
2MASS J04283018-6930502	67.125786	-69.513962	-6.732	-7.409	4.43
2MASS J05031358-6930326	75.806610	-69.509079	-7.471	-6.030	3.66
2MASS J05271416-6929112	81.809034	-69.486465	-6.920	-6.140	3.93
2MASS J05273189-6928353	81.882880	-69.476494	-6.614	-6.521	4.18
2MASS J05070471-6928053	76.769657	-69.468163	-7.720	-6.261	3.65
2MASS J05163771-6927142	79.157138	-69.453964	-7.160	-7.821	4.42
2MASS J04553354-6924593	73.889761	-69.416473	-10.266	-7.034	1.58
2MASS J05401333-6922464	85.055542	-69.379578	-9.988	-6.670	1.79
2MASS J05123400-6922086	78.141669	-69.369057	-7.455	-6.432	3.84
2MASS J04584149-6921314	74.672881	-69.358727	-6.960	-7.074	4.25
2MASS J04473884-6921170	71.911845	-69.354729	-8.041	-6.411	3.58
2MASS J06145902-6821262	93.745929	-68.357285	-7.088	-6.035	3.83
2MASS J05383397-6920317	84.641553	-69.342140	-10.082	-6.817	1.64
2MASS J05171633-6920298	79.318059	-69.341614	-8.005	-6.071	3.43
2MASS J05325547-6920266	83.231141	-69.340736	-6.864	-6.452	4.07
2MASS J05170066-6919304	79.252753	-69.325127	-7.770	-7.598	4.15
2MASS J05042995-6919235	76.124802	-69.323212	-7.291	-7.154	4.16
2MASS J05085218-6916337	77.217443	-69.276039	-7.114	-6.088	3.84
2MASS J05123206-6915404	78.133621	-69.261230	-7.602	-6.697	3.88
2MASS J05364101-6914064	84.170893	-69.235138	-9.293	-6.038	1.62
2MASS J04524566-6911494	73.190282	-69.197075	-8.631	-7.824	3.92
2MASS J04430510-6909128	70.771287	-69.153557	-7.530	-7.206	4.10
2MASS J05303638-6907099	82.651612	-69.119438	-9.715	-6.516	1.52
2MASS J05292199-6906584	82.341629	-69.116226	-7.729	-6.970	3.94
2MASS J05101432-6906103	77.559695	-69.102882	-7.222	-6.426	3.93
2MASS J05102724-6904532	77.613541	-69.081467	-6.994	-6.619	4.08
2MASS J05023218-6904377	75.634084	-69.077148	-6.885	-7.134	4.29
2MASS J05384137-6903540	84.672401	-69.065002	-7.076	-6.948	4.17
2MASS J05202143-6858479	80.089325	-68.979973	-6.628	-6.105	4.03
2MASS J04554180-6857227	73.924175	-68.956329	-7.858	-6.827	3.83
2MASS J05145597-6856464	78.733248	-68.946243	-6.756	-6.500	4.12
2MASS J05224292-6855288	80.678873	-68.924683	-7.653	-7.455	4.14
2MASS J05000498-6853553	75.020789	-68.898720	-9.182	-6.136	2.64
2MASS J04563215-6852510	74.133960	-68.880844	-7.466	-7.790	4.32
2MASS J05152176-6849019	78.840680	-68.817215	-7.409	-7.039	4.08
2MASS J05215630-6847225	80.484594	-68.789589	-6.969	-7.818	4.48
2MASS J05102834-6844313	77.618120	-68.742050	-7.244	-6.511	3.95
2MASS J04511548-6841403	72.814508	-68.694534	-7.498	-6.430	3.82
2MASS J05151758-6841198	78.823286	-68.688835	-6.811	-6.433	4.08
2MASS J04390199-6836322	69.758300	-68.608963	-7.050	-6.714	4.10
2MASS J04522647-6834374	73.110316	-68.577080	-9.619	-6.350	1.65

table continuation

2MASS ID	RA (deg)	Dec (deg)	M_K (mag)	M_{bol} (mag)	$J - K_s$ (mag)
2MASS J05565154-6827267	89.214751	-68.457420	-9.982	-6.665	1.79
2MASS J05474884-6825336	86.953524	-68.426003	-8.143	-6.340	3.49
2MASS J04471609-6824256	71.817052	-68.407120	-7.936	-6.677	3.74
2MASS J04552049-6822391	73.835412	-68.377541	-8.865	-6.074	2.88
2MASS J04554249-6816542	73.927067	-68.281723	-7.408	-6.360	3.83
2MASS J04585546-6813062	74.731110	-68.218407	-7.537	-6.276	3.74
2MASS J05325618-6812487	83.234091	-68.213539	-9.268	-6.358	2.78
2MASS J04544534-6804146	73.688926	-68.070747	-8.110	-6.008	3.34
2MASS J05081566-6800459	77.065279	-68.012764	-6.536	-6.002	4.02
2MASS J05213755-6752393	80.406488	-67.877594	-7.261	-6.149	3.80
2MASS J04594477-6752208	74.936568	-67.872452	-8.599	-6.264	3.20
2MASS J05111047-6752105	77.793643	-67.869591	-6.900	-8.385	4.66
2MASS J05502604-6749462	87.608526	-67.829506	-7.659	-6.966	3.97
2MASS J05214756-6749118	80.448169	-67.819962	-8.728	-6.123	3.03
2MASS J05100440-6745501	77.518363	-67.763939	-8.521	-6.009	3.09
2MASS J05150378-6744142	78.765788	-67.737289	-7.545	-6.310	3.75
2MASS J04553202-6742310	73.883426	-67.708626	-7.358	-7.068	4.11
2MASS J05195418-6739420	79.975765	-67.661674	-7.001	-6.063	3.87
2MASS J04333653-6739329	68.402242	-67.659157	-6.798	-7.252	4.36
2MASS J05065934-6734453	76.747273	-67.579254	-8.096	-6.033	3.36
2MASS J04521072-6734329	73.044681	-67.575813	-6.701	-6.414	4.11
2MASS J05503932-6731504	87.663860	-67.530685	-7.070	-7.581	4.38
2MASS J05342976-6730257	83.624008	-67.507164	-7.839	-6.198	3.57
2MASS J05054710-6727243	76.446275	-67.456772	-7.404	-8.260	4.48
2MASS J05135297-6726548	78.470730	-67.448563	-10.128	-6.799	1.85
2MASS J05081617-6723506	77.067413	-67.397408	-7.179	-6.069	3.80
2MASS J04572171-6721280	74.340464	-67.357780	-7.387	-6.021	3.69
2MASS J05281556-6720188	82.064839	-67.338562	-7.590	-6.745	3.91
2MASS J05283913-6718089	82.163055	-67.302483	-6.798	-6.499	4.11
2MASS J04542493-6709344	73.603899	-67.159569	-7.291	-7.640	4.32
2MASS J05001899-6707580	75.079159	-67.132782	-9.267	-6.234	2.66
2MASS J05323716-6706564	83.154849	-67.115669	-7.943	-6.586	3.70
2MASS J04352409-6656493	68.850409	-66.947029	-6.874	-6.835	4.20
2MASS J04545344-6651375	73.722698	-66.860435	-8.841	-6.201	3.00
2MASS J05113864-6651098	77.911028	-66.852730	-7.853	-6.151	3.54
2MASS J04253216-6647163	66.384027	-66.787888	-7.505	-6.941	4.01
2MASS J05062118-6643161	76.588262	-66.721153	-6.932	-7.655	4.44
2MASS J06085255-6727472	92.218968	-67.463135	-7.407	-6.352	3.82
2MASS J05365212-6631004	84.217194	-66.516792	-7.317	-6.745	4.01
2MASS J04433797-6628577	70.908249	-66.482704	-7.934	-6.141	3.50
2MASS J05383208-6615382	84.633676	-66.260620	-8.882	-6.231	2.99
2MASS J05311311-6609411	82.804646	-66.161438	-7.045	-6.932	4.17
2MASS J04512141-6609328	72.839233	-66.159134	-7.513	-6.138	3.69
2MASS J05385059-6609200	84.710828	-66.155571	-8.543	-6.284	3.25
2MASS J05320136-6603279	83.005668	-66.057762	-7.634	-6.406	3.75
2MASS J05100176-6551565	77.507357	-65.865715	-7.153	-6.289	3.90
2MASS J04555834-6544052	73.993113	-65.734795	-9.244	-6.019	2.39
2MASS J05225895-6544029	80.745639	-65.734154	-7.436	-7.157	4.12
2MASS J04444769-6537072	71.198747	-65.618690	-7.080	-7.329	4.29
2MASS J05280808-6535201	82.033687	-65.588928	-8.207	-6.633	3.60
2MASS J05242363-6532107	81.098476	-65.536324	-7.462	-6.007	3.66
2MASS J04470329-6524563	71.763718	-65.415649	-6.761	-7.474	4.44

table continuation

2MASS ID	RA (deg)	Dec (deg)	M_K (mag)	M_{bol} (mag)	$J - K_s$ (mag)
2MASS J05524672-6520071	88.194668	-65.335320	-6.935	-7.064	4.25
2MASS J05353972-6519564	83.915505	-65.332336	-6.717	-6.018	3.96
2MASS J05121594-6518431	78.066420	-65.311981	-7.344	-6.286	3.82
2MASS J05275737-6517363	81.989046	-65.293442	-7.775	-6.799	3.86
2MASS J05295356-6514567	82.473182	-65.249100	-7.415	-6.485	3.87
2MASS J05403844-6457245	85.160171	-64.956818	-7.480	-7.262	4.14
2MASS J05164004-6439127	79.166850	-64.653542	-7.921	-7.117	3.92
2MASS J05501757-6428545	87.573216	-64.481812	-8.407	-6.115	3.23
2MASS J05340710-6416479	83.529602	-64.279976	-7.959	-6.297	3.56
2MASS J05123875-6412136	78.161467	-64.203796	-8.960	-6.589	3.18
2MASS J05310498-6408306	82.770769	-64.141853	-8.952	-6.505	3.13
2MASS J05255025-6400090	81.459387	-64.002502	-8.114	-6.064	3.37
2MASS J05273859-6330540	81.910813	-63.515015	-7.055	-7.599	4.39
2MASS J05152379-6321528	78.849158	-63.364693	-6.960	-6.736	4.13
2MASS J07193710-6559010	109.904590	-65.983627	-7.339	-6.559	3.93

Table A.2. Very luminous AGB stars (carbon star candidates) in the SMC

2MASS ID	RA (deg)	Dec (deg)	M_K (mag)	M_{bol} (mag)	$J - K_s$ (mag)
2MASS J00365957-7419503	9.248213	-74.330643	-9.886	-6.564	2.14
2MASS J01020652-7404291	15.527175	-74.074753	-8.164	-6.114	3.37
2MASS J00562548-7400468	14.106208	-74.013023	-7.764	-6.071	3.55
2MASS J00404385-7345244	10.182728	-73.756790	-7.558	-7.911	4.33
2MASS J00485947-7335387	12.247813	-73.594093	-7.889	-7.729	4.16
2MASS J00500719-7331251	12.529961	-73.523666	-10.381	-7.437	2.75
2MASS J00403293-7328399	10.137230	-73.477760	-7.453	-6.860	4.00
2MASS J00570590-7326518	14.274601	-73.447746	-8.337	-6.363	3.41
2MASS J00470552-7321330	11.773011	-73.359169	-8.700	-6.173	3.08
2MASS J01081031-7315524	17.042983	-73.264565	-9.432	-6.208	1.56
2MASS J01030900-7313583	15.787516	-73.232887	-7.260	-7.402	4.26
2MASS J00474454-7313072	11.935618	-73.218681	-8.607	-6.685	3.43
2MASS J00411442-7310091	10.310122	-73.169220	-7.046	-7.133	4.24
2MASS J00372080-7309447	9.336667	-73.162430	-7.173	-6.981	4.15
2MASS J00430955-7309223	10.789804	-73.156219	-8.230	-6.134	3.34
2MASS J00485250-7308568	12.218778	-73.149124	-7.905	-6.197	3.54
2MASS J00545410-7303181	13.725440	-73.055054	-8.235	-6.485	3.52
2MASS J00494271-7302207	12.427986	-73.039093	-7.144	-6.136	3.84
2MASS J00424090-7257057	10.670455	-72.951599	-8.857	-6.236	3.01
2MASS J00572770-7253279	14.365420	-72.891106	-7.159	-6.634	4.03
2MASS J00450214-7252243	11.258941	-72.873428	-7.828	-7.414	4.07
2MASS J00503062-7251298	12.627616	-72.858299	-10.237	-7.044	1.51
2MASS J00524017-7247276	13.167399	-72.791023	-9.174	-6.085	2.59
2MASS J00542228-7243296	13.592872	-72.724907	-7.307	-7.554	4.29
2MASS J01051049-7240563	16.293740	-72.682327	-7.115	-6.788	4.10
2MASS J00462352-7237397	11.598031	-72.627708	-7.306	-6.356	3.87
2MASS J00591577-7227546	14.815710	-72.465179	-8.049	-6.434	3.58
2MASS J00472059-7225360	11.835832	-72.426689	-7.010	-7.561	4.39

table continuation

2MASS ID	RA (deg)	Dec (deg)	M_K (mag)	M_{bol} (mag)	$J - K_s$ (mag)
2MASS J00510074-7225185	12.753117	-72.421829	-8.031	-6.679	3.70
2MASS J01122496-7220248	18.104013	-72.340225	-7.176	-7.542	4.33
2MASS J00432514-7218511	10.854768	-72.314217	-9.343	-6.026	2.17
2MASS J01003166-7214489	15.131924	-72.246941	-8.041	-6.111	3.43
2MASS J00465078-7147393	11.711623	-71.794250	-7.560	-6.015	3.61
2MASS J00322809-7147207	8.117061	-71.789093	-7.673	-6.391	3.73

Table A.3. Very luminous AGB stars (carbon star candidates) in M31

2MASS ID	RA (deg)	Dec (deg)	M_K (mag)	M_{bol} (mag)	$J - K_s$ (mag)
2MASS J00394632+4030280	9.943011	40.507805	-10.339	-7.083	1.62
2MASS J00422751+4035524	10.614644	40.597908	-9.834	-6.591	1.60
2MASS J00452772+4035589	11.365515	40.599712	-9.514	-6.325	1.50
2MASS J00405951+4036490	10.247993	40.613636	-11.009	-7.727	1.68
2MASS J00405912+4036536	10.246338	40.614906	-10.819	-7.591	1.57
2MASS J00410100+4037072	10.254204	40.618690	-9.944	-6.668	1.67
2MASS J00410122+4037321	10.255102	40.625584	-10.320	-7.055	1.64
2MASS J00413945+4037416	10.414384	40.628242	-9.646	-6.392	1.62
2MASS J00411799+4040170	10.324980	40.671394	-10.198	-6.999	1.52
2MASS J00414753+4040588	10.448079	40.683018	-9.645	-6.429	1.55
2MASS J00405497+4044108	10.229067	40.736359	-10.713	-7.413	1.73
2MASS J00405619+4045461	10.234160	40.762817	-11.136	-7.919	1.55
2MASS J00421697+4047487	10.570731	40.796864	-10.310	-6.976	2.08
2MASS J00412184+4050090	10.341023	40.835857	-10.957	-7.708	1.61
2MASS J00414909+4050485	10.454579	40.846828	-9.736	-6.405	1.86
2MASS J00402901+4050485	10.120903	40.846828	-9.907	-6.717	1.50
2MASS J00424499+4051349	10.687467	40.859707	-10.687	-7.432	1.62
2MASS J00415135+4052139	10.463964	40.870552	-9.523	-6.315	1.53
2MASS J00404426+4054039	10.184426	40.901096	-9.651	-6.452	1.52
2MASS J00404649+4055220	10.193716	40.922802	-10.666	-7.445	1.56
2MASS J00424067+4059225	10.669477	40.989601	-9.542	-6.306	1.58
2MASS J00424586+4059583	10.691123	40.999554	-10.352	-7.136	1.55
2MASS J00401171+4101138	10.048817	41.020523	-10.045	-6.731	1.78
2MASS J00404879+4102304	10.203307	41.041782	-9.769	-6.579	1.50
2MASS J00440117+4104054	11.004878	41.068172	-9.585	-6.369	1.55
2MASS J00413891+4104262	10.412128	41.073956	-10.788	-7.459	2.11
2MASS J00410868+4104383	10.286197	41.077316	-10.902	-7.586	2.17
2MASS J00414286+4107300	10.428614	41.125015	-9.872	-6.671	1.52
2MASS J00434139+4109384	10.922468	41.160683	-9.630	-6.365	1.64
2MASS J00412777+4109388	10.365709	41.160801	-9.681	-6.456	1.56
2MASS J00412030+4111073	10.334590	41.185371	-9.927	-6.712	1.55
2MASS J00434371+4111258	10.932143	41.190514	-10.117	-6.831	1.69
2MASS J00434135+4112137	10.922321	41.203815	-10.265	-7.036	1.57
2MASS J00433662+4112152	10.902587	41.204224	-9.793	-6.553	1.59
2MASS J00405596+4112152	10.233187	41.204247	-9.646	-6.423	1.56
2MASS J00434617+4112331	10.942393	41.209213	-9.952	-6.618	1.88
2MASS J00434686+4112451	10.945257	41.212532	-10.839	-7.615	1.56

table continuation

2MASS ID	RA (deg)	Dec (deg)	M_K (mag)	M_{bol} (mag)	$J - K_s$ (mag)
2MASS J00435338+4113016	10.972420	41.217136	-11.022	-7.682	1.95
2MASS J00435217+4114228	10.967414	41.239681	-9.583	-6.307	1.67
2MASS J00424061+4115009	10.669212	41.250271	-11.215	-7.952	1.64
2MASS J00441547+4116071	11.064496	41.268646	-9.388	-6.179	1.53
2MASS J00440575+4117199	11.023975	41.288864	-10.343	-7.139	2.43
2MASS J00440440+4117260	11.018359	41.290573	-10.537	-7.197	2.00
2MASS J00414297+4117300	10.429050	41.291691	-10.946	-7.652	1.71
2MASS J00414817+4118332	10.450715	41.309223	-9.873	-6.613	1.63
2MASS J00441789+4119230	11.074565	41.323059	-10.849	-7.612	1.58
2MASS J00441402+4121420	11.058431	41.361691	-10.121	-6.899	1.56
2MASS J00442322+4121496	11.096773	41.363789	-9.974	-6.635	1.93
2MASS J00442890+4121589	11.120435	41.366371	-9.809	-6.470	1.93
2MASS J00443503+4123585	11.145990	41.399609	-9.559	-6.336	1.56
2MASS J00415182+4124420	10.465925	41.411690	-10.568	-7.342	1.56
2MASS J00443680+4124465	11.153358	41.412933	-11.078	-7.739	2.02
2MASS J00443163+4125579	11.131823	41.432758	-9.911	-6.702	1.53
2MASS J00405722+4127239	10.238433	41.456665	-9.710	-6.468	1.59
2MASS J00443076+4128352	11.128191	41.476463	-10.435	-7.217	1.55
2MASS J00423161+4129146	10.631723	41.487389	-10.476	-7.211	1.64
2MASS J00445416+4129530	11.225678	41.498062	-10.214	-6.989	1.56
2MASS J00444232+4130556	11.176369	41.515465	-9.295	-6.074	1.56
2MASS J00450163+4131148	11.256814	41.520779	-11.079	-7.884	1.51
2MASS J00445845+4131352	11.243563	41.526451	-10.523	-7.288	1.58
2MASS J00424172+4132501	10.673849	41.547260	-10.530	-7.268	2.32
2MASS J00424417+4133040	10.684061	41.551125	-10.199	-6.861	2.04
2MASS J00423133+4133103	10.630557	41.552876	-10.480	-7.149	2.10
2MASS J00451065+4133248	11.294379	41.556915	-9.826	-6.490	1.90
2MASS J00441105+4133354	11.046080	41.559841	-10.288	-7.059	1.57
2MASS J00423774+4135395	10.657289	41.594326	-9.745	-6.453	1.71
2MASS J00451348+4136308	11.306202	41.608582	-10.546	-7.229	1.79
2MASS J00425798+4137099	10.741592	41.619442	-9.524	-6.279	1.60
2MASS J00430247+4137386	10.760300	41.627399	-10.649	-7.389	1.63
2MASS J00430142+4137423	10.755923	41.628422	-10.393	-7.150	1.60
2MASS J00430151+4137551	10.756292	41.631985	-10.597	-7.297	1.73
2MASS J00430776+4138124	10.782355	41.636780	-10.488	-7.261	1.57
2MASS J00451834+4139220	11.326427	41.656124	-9.708	-6.442	1.64
2MASS J00432196+4141126	10.841507	41.686848	-9.919	-6.639	1.68
2MASS J00445355+4141357	11.223136	41.693253	-9.497	-6.279	1.55
2MASS J00454539+4142352	11.439165	41.709801	-9.465	-6.240	1.56
2MASS J00451861+4143201	11.327579	41.722263	-10.017	-6.784	1.58
2MASS J00434203+4144032	10.925149	41.734238	-9.785	-6.493	1.71
2MASS J00435943+4146429	10.997627	41.778587	-9.328	-6.131	1.52
2MASS J00440219+4147493	11.009132	41.797043	-10.116	-6.917	1.52
2MASS J00441497+4148529	11.062387	41.814697	-9.513	-6.319	1.51
2MASS J00425297+4149210	10.720725	41.822521	-9.685	-6.493	1.51
2MASS J00440179+4149236	11.007496	41.823238	-9.561	-6.339	1.56
2MASS J00440685+4149571	11.028579	41.832550	-9.483	-6.294	1.50
2MASS J00445634+4149579	11.234758	41.832775	-9.519	-6.277	1.59
2MASS J00454261+4150058	11.427546	41.834961	-9.937	-6.667	1.65
2MASS J00442653+4150557	11.110566	41.848827	-10.102	-6.771	1.86
2MASS J00442081+4151597	11.086717	41.866611	-11.269	-8.068	1.52
2MASS J00443048+4152231	11.127036	41.873104	-10.714	-7.451	1.64

table continuation

2MASS ID	RA (deg)	Dec (deg)	M_K (mag)	M_{bol} (mag)	$J - K_s$ (mag)
2MASS J00444915+4152273	11.204827	41.874271	-11.053	-7.802	1.61
2MASS J00443153+4153031	11.131396	41.884197	-10.354	-7.142	1.54
2MASS J00453263+4153356	11.385993	41.893234	-9.550	-6.362	1.50
2MASS J00451817+4153503	11.325713	41.897324	-9.580	-6.387	1.51
2MASS J00441502+4154102	11.062585	41.902859	-9.431	-6.186	1.60
2MASS J00443323+4154382	11.138468	41.910625	-9.529	-6.255	1.66
2MASS J00443446+4154487	11.143602	41.913532	-9.557	-6.246	1.77
2MASS J00444960+4154503	11.206699	41.913990	-9.482	-6.281	1.52
2MASS J00452458+4155249	11.352445	41.923588	-9.749	-6.522	1.57
2MASS J00443676+4155300	11.153187	41.925011	-9.749	-6.515	1.58
2MASS J00453432+4158096	11.393025	41.969357	-9.835	-6.617	1.55

Table A.4. Very luminous AGB stars (carbon star candidates) in M33

2MASS ID	RA (deg)	Dec (deg)	M_K (mag)	M_{bol} (mag)	$J - K_s$ (mag)
2MASS J01331769+3021253	23.323723	30.357054	-9.970	-6.735	1.58
2MASS J01335587+3027285	23.482809	30.457930	-10.630	-7.341	1.70
2MASS J01330404+3013225	23.266844	30.222937	-9.714	-6.399	1.78
2MASS J01323279+3030250	23.136661	30.506952	-9.829	-6.489	1.95
2MASS J01340022+3040475	23.500920	30.679874	-10.369	-7.064	1.75
2MASS J01335459+3040262	23.477486	30.673952	-10.671	-7.340	1.86
2MASS J01340697+3047539	23.529077	30.798306	-10.084	-6.803	1.68
2MASS J01340090+3034465	23.503776	30.579611	-9.948	-6.759	1.50
2MASS J01333366+3033204	23.390251	30.555672	-9.750	-6.472	1.67
2MASS J01341556+3052499	23.564865	30.880529	-10.932	-7.592	2.01
2MASS J01333418+3041271	23.392448	30.690870	-10.598	-7.281	1.79
2MASS J01335855+3033525	23.493967	30.564590	-9.540	-6.331	1.54
2MASS J01335488+3038537	23.478687	30.648275	-9.900	-6.594	1.75
2MASS J01333862+3032254	23.410958	30.540401	-10.196	-6.891	1.75
2MASS J01334194+3038565	23.424778	30.649031	-10.520	-7.301	1.55
2MASS J01334389+3032246	23.432910	30.540171	-10.020	-6.763	1.63
2MASS J01335316+3038389	23.471534	30.644152	-10.157	-6.897	1.63
2MASS J01333357+3031599	23.389879	30.533327	-10.884	-7.555	2.11
2MASS J01334172+3050390	23.423867	30.844172	-9.993	-6.656	1.91
2MASS J01332901+3042541	23.370907	30.715054	-9.587	-6.324	1.64
2MASS J01340652+3054510	23.527172	30.914177	-10.135	-6.795	2.00
2MASS J01334812+3039301	23.450541	30.658377	-9.842	-6.617	1.56
2MASS J01340055+3059387	23.502324	30.994099	-9.748	-6.462	1.69
2MASS J01341459+3033543	23.560816	30.565096	-10.211	-6.985	1.57
2MASS J01355238+3051030	23.968257	30.850855	-9.520	-6.295	1.56
2MASS J01350167+3054534	23.756997	30.914835	-10.324	-7.042	1.68
2MASS J01340739+3035173	23.530827	30.588150	-9.636	-6.343	1.71
2MASS J01323260+3030567	23.135842	30.515766	-9.592	-6.394	1.52
2MASS J01323983+3038170	23.165985	30.638075	-9.556	-6.308	1.61
2MASS J01330147+3033361	23.256127	30.560051	-10.030	-6.788	1.60
2MASS J01321356+3040033	23.056537	30.667587	-9.520	-6.327	1.51